HHS Public Access

Author manuscript

Science. Author manuscript; available in PMC 2021 May 01.

Published in final edited form as:

Science. 2020 May 01; 368(6490): . doi:10.1126/science.aat3987.

Interleukin 13 drives metabolic conditioning of muscle to endurance exercise

Nelson H. Knudsen[1], **Kristopher J. Stanya**[1], **Alexander L. Hyde**[1], **Mayer M. Chalom**[1], **Ryan K. Alexander**[1], **Yae-Huei Liou**[1], **Kyle A. Starost**[1], **Matthew R. Gangl**[1], **David Jacobi**[1,2], **Sihao Liu**[1,3], **Danesh H. Sopariwala**[4], **Diogo Fonseca-Pereira**[5], **Jun Li**[6], **Frank B. Hu**[6,7], **Wendy S. Garrett**[1,5], **Vihang Narkar**[4], **Eric A. Ortlund**[8], **Jonathan H. Kim**[8,9], **Chad M. Paton**[10], **Jamie A. Cooper**[10], **Chih-Hao Lee**[1,*]

[1]Department of Molecular Metabolism, Harvard T.H. Chan School of Public Health, 665 Huntington Ave, Boston, MA 02115, USA

[2]Current address: l'institut du thorax, INSERM, CNRS, UNIV Nantes & CHU Nantes, Nantes, France

[3]Current address: Ionis Pharmaceuticals, 2855 Gazelle Ct, Carlsbad, CA 92110, USA

[4]Metabolic and Degenerative Diseases, Institute of Molecular Medicine, The University of Texas McGovern Medical School, Houston, TX 77030, USA

[5]Department of Immunology and Infectious Diseases, Harvard T.H. Chan School of Public Health, 665 Huntington Ave, Boston, MA 02115, USA

[6]Department of Nutrition and Department of Epidemiology, Harvard T.H. Chan School of Public Health, 665 Huntington Ave, Boston, MA 02115, USA

[7]Channing Division of Network medicine, Department of Medicine, Brigham and Women's Hospital and Harvard Medical School, Boston, MA

[8]Emory University School of Medicine, Atlanta, GA 30322, USA

[9]Emory Clinical Cardiovascular Research Institute, Atlanta, GA 30322, USA

[10]Department of Foods and Nutrition, University of Georgia, Athens, GA 30602, USA

[*]Correspondence should be addressed: C.-H. L. clee@hsph.harvard.edu, Department of Molecular Metabolism, Harvard T.H. Chan School of Public Health, 665 Huntington Ave, Bldg1, Rm 409, Boston, MA 02115, USA. Phone: +1(617) 432-5778.

Author contributions: N.H.K., K.J.S., A.L.H., M.M.C., R.K.A., Y.H.L., K.A.S, M.R.G., D.J., S.L. performed the experiments. E.A.O., J.H.K., C.M.P., and J.A.C. provided human plasma samples. D.H.S. and V.N. assisted in electron microscopy analysis and method development. D.F.P. and W.S.G. assisted in flow cytometry analysis of ILCs. L.J and F.B.H were consulted for analyses related to RNA-seq and human plasma data and provided recommendations for statistical methods. N.H.K. and C.H.L. conceptualized the study, designed experiments, interpreted data and wrote the manuscript. C.H.L. supervised the study.

Competing interests: Authors declare no competing interests.

Data and materials availability: RNA-sequencing data from this study have been deposited in GEO under the accession number GSE126001.

Supplementary Materials:
Materials and Methods
Figures S1–S6
Tables S1–S5
External Data S1–S3

Abstract

Repeated bouts of exercise condition muscle mitochondria to meet increased energy demand, an adaptive response associated with improved metabolic fitness. We find that the type 2 cytokine interleukin-13 (IL-13) is induced in exercising muscle, where it orchestrates metabolic reprogramming that preserves glycogen in favor of fatty acid oxidation and mitochondrial respiration. Exercise training-mediated mitochondrial biogenesis, running endurance, and beneficial glycemic effects are lost in *Il13*$^{-/-}$ mice. By contrast, enhanced muscle IL-13 signaling is sufficient to increase running distance, glucose tolerance, and mitochondrial activity similar to that of exercise training. IL-13 acts through both muscle IL-13Rα1 and Stat3. The genetic ablation of either of these downstream effectors reduces running capacity. Thus, coordinated immunological and physiological responses mediate exercise-elicited metabolic adaptations that maximize muscle fuel economy.

One Sentence Summary:

Endurance exercise activates IL-13 signaling to regulate muscle mitochondrial oxidative capacity and glucose homeostasis.

Exercise reduces the risk of multiple diseases, notably metabolic syndrome. Many beneficial effects of regular exercise occur independently of body weight changes (1). Early studies implicated unidentified humoral factors that mediate insulin-independent, exercise-induced muscle glucose uptake (2). Subsequently, several “myokines” or muscle-produced factors have been reported (3). IL-6 is one of the first myokines described to be acutely induced after exercise. In vitro studies suggested that IL-6 enhances glucose utilization in differentiated myotubes (3). However, resting IL-6 levels are actually reduced by endurance training and increased in obesity (3). Furthermore, *Il6* gene deletion in mice does not affect glucose uptake, substrate metabolism, or running capacity, suggesting that additional factors are involved in metabolic adaptations to prolonged physical activity (4, 5).

IL-13 is an exercise-induced regulator of endurance capacity

To better understand the immunological response and identify circulating factors elicited by endurance exercise, we profiled a panel of human type 1 and 2 cytokines in plasma from obese, normal-weight sedentary, and endurance-trained women (performing >1 hour of aerobic exercise at least four times per week). Consistent with prior reports, obese female participants had higher plasma IL-6 levels (Fig. 1A and table S1). Endurance-trained women had significantly higher IL-13, but lower IL-6 levels (Fig. 1A and table S1). In a separate cohort of normal-weight sedentary men, college cross-country runners, and American-football players (samples collected post-season), male athletes had significantly higher plasma IL-13 levels but showed no differences in IL-6 levels, compared to controls (Fig. 1B). We observed similar (albeit non-statistically significant) trends for higher IL-13 and lower IL-6 circulating concentrations when female or male mice subjected to 4–5 weeks of endurance training (40-min low-intensity treadmill running daily, 5 days per week) were compared to untrained controls (fig. S1, A and B). Exercise is reported to increase myokine production. However, *Il13* mRNA was not detectable in mouse primary myotubes but

enriched in Percoll-isolated immune and stromal cells from muscle lysate (Fig. 1C). Exercise training further upregulated *Il13* expression in these cells (Fig. 1D). The myokine *Il6* was expressed in both myotubes and muscle immune/stromal cells. Its expression was not affected by exercise. A primary source of IL-13 is tissue resident type 2 innate lymphoid cells (ILC2s) (6). After 4 weeks of endurance training, the percentage of ILC2 in the $Cd45^+$ cell population was significantly increased, whereas the percentage of ILC3 or T cells did not change (Fig. 1E and fig. S1C). In addition, among $CD45^+$ cells, ILC2s constituted a greater percentage of IL-13-producing cells than T cells (Fig. 1F). A well characterized activator of ILC2 is IL-33, which is produced by multipotent stromal cells (MSC) in skeletal muscle and adipose tissue (7–10). In mice, serum IL-33 concentrations increased following one bout of exercise and remained elevated for at least 2 hours (fig. S1D). Treatment with IL-33 or phorbol myristate acetate plus ionomycin upregulated *Il13* expression in muscle immune/stromal cells (fig. S1E). Thus, ILC2s in skeletal muscle may service as a source of IL-13 producing cells activated by endurance exercise.

To examine the relevance of IL-13 in exercise physiology, we performed treadmill-running tests comparing WT and *Il13* whole-body–knockout ($Il13^{-/-}$) mice. $Il13^{-/-}$ mice displayed a significant reduction in running time and distance (Fig. 1G). However, there were no differences in their muscle strength, compared to WT controls (fig. S1F). Similar results were observed for both male and female mice. Data presented are primarily from male mice unless stated otherwise. Thus, IL-13 is a candidate humoral factor induced by endurance training that modulates running capacity.

IL-13 regulates energy substrate utilization during endurance exercise

To determine the molecular basis of IL-13 signaling in regulating exercise physiology, we performed mRNA expression profiling by RNA-sequencing (RNA-seq) using gastrocnemius muscle samples from WT control and $Il13^{-/-}$ mice with or without exercise training as described earlier. Exercise training significantly upregulated the expression of 155 genes and downregulated 81 genes in skeletal muscle of WT mice (*FDR*<0.05). However, only two of these genes were similarly regulated by exercise training in muscle of $Il13^{-/-}$ mice (fig. S2A). A similar discordance was observed among genes nominally (*P*<0.05) regulated by exercise when comparing WT with $Il13^{-/-}$ mice (fig. S2A). We therefore included differentially expressed genes with *P*<0.05 in gene ontology analysis to ensure sufficient power for identifying enriched biological functions. Gene ontology enrichment analyses identified fatty acid/lipid metabolism (*FDR-enrichment*<0.05) and tricarboxylic acid (TCA) cycle (*FDR-enrichment*=0.056) among the most upregulated biological processes, comparing exercise-trained WT mice with untrained WT controls (fig. S2B and data S1). Differential expression of selected key genes in these biological processes could be validated by real-time quantitative PCR (qPCR, fig. S2C). Among the genes upregulated by exercise training in muscle of WT mice were those involved in fatty acid uptake (e.g., lipoprotein lipase (*Lpl*) and acyl-coA synthetase long-chain family member 1 (*Acsl1*)), fatty acid beta oxidation (e.g., carnitine palmitoyltransferase 1b (*Cpt1b*) and acyl-coA dehydrogenase very long chain (*Acadvl*)) and TCA cycle enzymes (e.g., pyruvate dehydrogenase alpha 1 (*Pdha1*) and isocitrate dehydrogenase 2 (*Idh2*)) (Fig. 2A). In addition, glycogen branching enzyme (*Gbe1*) (required for glycogen synthesis) and lactate dehydrogenase b (*Ldhb*) (an enzyme

converting lactate to pyruvate for entrance into the TCA cycle) were also increased in exercised muscle. By contrast, glycogenolysis (e.g., phosphorylase kinase subunit gamma 1 (*Phkg1*)) was among the major biological processes downregulated by endurance exercise in WT muscle (Fig. 2A and fig. S2, B and C). This agrees with the notion that endurance running preserves muscle glycogen stores and promotes a metabolic switch from glycolysis to fatty acid oxidation (11). However, this metabolic reprogramming was lost in *Il13*$^{-/-}$ mice.

Consistent with the RNA-seq data, recombinant IL-13 (rIL-13) increased fatty acid uptake, β-oxidation, and glucose uptake in differentiated C2C12 myotubes (Fig. 2, B and C) with similar results observed in primary myotubes (fig. S2D). Single bouts of acute exercise without exhaustion (30 min, 12 m/min) were used to examine the role of IL-13 in muscle substrate utilization in vivo. WT mice had significantly lower intramuscular triglyceride (TG, quadriceps) and maintained glycogen levels after exercise (Fig. 2D). Mice lacking *Il13* had reduced muscle glycogen content, whereas TG content was unchanged. Muscle TG and glycogen levels did not differ between WT and *Il13*$^{-/-}$ mice at resting state. Serum free fatty acid (FFA), triglyceride (TG), and glycerol levels were similarly elevated by exercise in both genotypes (Fig. 2E). This suggests that the exercise-elicited defect in *Il13*$^{-/-}$ mice was muscle-intrinsic and not at the substrate level. Using an enclosed metabolic treadmill chamber in a running test, we determined that *Il13*$^{-/-}$ mice had lower maximal oxygen uptake (VO_2 max) (Fig. 2F), consistent with their reduced running capacity (Fig. 1G). Muscle structure and mass were similar between WT and *Il13*$^{-/-}$ mice (fig. S2, E and F). There was no significant difference in the basal oxygen consumption rate between untrained or trained WT and *Il13*$^{-/-}$ mice (5 months old, fig. S2G). Thus, IL-13 plays a role in regulating the metabolic substrates that fuel exercising muscle.

Exercise training-induced muscle mitochondrial biogenesis and glucose tolerance require IL-13

Endurance training increases mitochondrial oxidative metabolism by increasing both mitochondrial biogenesis and respiratory capacity. For genes differentially expressed in muscle of WT and *Il13*$^{-/-}$ mice, gene ontology analysis further identified oxidation reduction as a key biological process dysregulated in *Il13*$^{-/-}$ muscle (*FDR-enrichment*<0.05), in addition to fatty acid metabolism, especially under trained conditions (fig. S3A, and data S2). Most genes in this category belonged to mitochondrial oxidative metabolism that were also upregulated by endurance exercise in WT mice (Fig. 3A and fig. S3B). These included genes involved in the electron transfer flavoprotein, mitochondrial ribosome, mitochondrial protein import, and components of the electron transport chain (ETC) complexes. The expression of these genes was either unchanged or instead downregulated by exercise training in *Il13*$^{-/-}$ mice.

In C2C12 myotubes, rIL-13 treatment led to higher basal and maximal mitochondrial oxygen consumption rate. This was accompanied by an increase in mitochondrial biogenesis determined by the ratio of mitochondrial DNA (mtDNA) to nuclear DNA (Fig. 3B). Similar results were observed in primary myotubes (fig. S3C). By contrast, rIL-6 failed to promote

respiration (fig. S3D). Consistent with the RNA-seq results, endurance training increased mitochondrial ETC complex proteins in the gastrocnemius muscle of WT but not *Il13*$^{-/-}$ mice (Fig. 3C). Electron microscopy further demonstrated that endurance exercise increased the average muscle mitochondrial area in WT mice (fig. S3E). *Il13*$^{-/-}$ muscle mitochondrial area was not altered by exercise. Endurance training also promoted a shift in muscle fiber type composition towards increased oxidative fibers (types I and IIa; succinate dehydrogenase activity-positive) and reduced glycolytic fibers (types IIb and IIx) in WT but not *Il13*$^{-/-}$ mice (Fig. 3, D and E, and fig. S3, F and G). These changes were associated with IL-13-dependent increases in muscle mitochondrial respiration when the complex II and IV substrates—succinate and ascorbate/tetramethyl-*p*-phenylenediamine, respectively—were used (Fig. 4A). Similar results were obtained for complex IV activity (Fig. 4B). In addition, endurance training increased the running capacity and glucose tolerance of WT male (Fig. 4, C and D) and female mice (fig. S4, A and B), compared to untrained animals. This training-induced increase in metabolic fitness was lost in *Il13*$^{-/-}$ mice. Thus, although IL-13 signaling is dispensable for basal mitochondrial respiration, it is necessary to increase muscle mitochondrial biogenesis and oxidative capacity and enhance systemic glucose homeostasis in response to exercise training.

The IL-13Rα1–Stat3 axis mediates IL-13 activity in muscle

IL-13 signals via a heterodimeric receptor composed of IL-13Rα1 and IL-4R. Knockdown of *Il13ra1* in C2C12 myotubes blocked rIL-13-mediated increases in mitochondrial respiration (fig. S5A). Similar to *Il13*$^{-/-}$ mice, whole-body *Il13ra1*–knockout (*Il13ra1*$^{-/-}$) mice had reduced endurance running capacity (Fig. 5A). Subsequently, skeletal muscle-specific *Il13ra1*–knockout (skm*Il13ra1*$^{-/-}$) mice were generated by crossing *Il13ra1*$^{f/f}$ allele with *ACTA1*-cre mice (fig. S5B). skm*Il13ra1*$^{-/-}$ mice retained normal muscle weight/morphology (fig. S5, C and D), but had a significant reduction in endurance running capacity and muscle fatty acid oxidation (Fig. 5B). Stat6 is the canonical transcription factor mediating transcription downstream of IL-13 receptors in immune cells. However, it is not expressed in muscle. De novo motif analysis of the promoters of mitochondrial genes differentially regulated in muscle of exercise trained WT and *Il13*$^{-/-}$ mice identified several enriched binding sites for transcription factors, such as the Err nuclear receptors and Stat3 (Fig. S5E and data S3). Activation of Stat3 through Jak signaling downstream of IL-13Rα1 has been described in other cell types, including hepatocytes (12, 13). Stat3 phosphorylation was elevated in muscle after both a single session and endurance training (fig. S5F and Fig. 5C), an effect lost upon *Il13* deletion. In concert, muscle IL-13 protein levels were increased by one exercise session and, to a greater extent, by endurance training (fig. S5G, IL-13 protein increase in single session exercise was not significant). rIL-13 treatment in C2C12 myotubes directly increased Stat3 phosphorylation, whereas *Stat3* knockdown blocked rIL-13-induced mitochondrial respiration (fig. S5, H and I). Skeletal muscle–specific *Stat3*–knockout (skm*Stat3*$^{-/-}$) mice, generated by crossing *Stat3*$^{f/f}$ (control) to *ACTA1*-cre mice (fig. S5, J and K), also ran less and had reduced soleus muscle fatty acid β-oxidation (Fig. 5D), similar to *Il13*$^{-/-}$, *Il13ra1*$^{-/-}$, and skm*Il13ra1*$^{-/-}$ mice.

Elevated IL-13 signaling in muscle confers an endurance training-like effect

To examine the dependence of IL-13 signaling on muscle Stat3, intramuscular injection of adenoviral IL-13 (adIL-13; adGFP was used as a control) was employed to increase IL-13 levels in skeletal muscle. Injection of adIL-13 into gastrocnemius muscle (fig. S6, A and B) induced Stat3 phosphorylation (as well as total Stat3 protein) in uninjected quadriceps muscle (fig. S6C), with concomitant increases in quadriceps and serum IL-13 levels (fig. S6D) and without altering muscle mass (fig. S6E). Elevated IL-13 signaling in muscle through gastrocnemius adIL-13 injection was sufficient to regulate the expression of exercise-controlled genes identified by RNA-seq (fig. S6F), increase respiration of isolated mitochondria given substrates for complexes II and IV (fig. S6G), enhance treadmill running time and distance and soleus muscle fatty acid oxidation (Fig. 6A), and improve glucose tolerance in WT mice (Fig. 6B). These effects were completely abolished in skm*Stat3*$^{-/-}$ mice. Thus, IL-13 activates muscle Stat3 to regulate mitochondrial oxidative metabolism during exercise. In addition, increasing IL-13 signaling locally in the muscle drives an exercise-like effect on mitochondrial activity that is accompanied by increased running capacity and glucose tolerance.

The motif enrichment analysis indicated that the Err nuclear receptor family, which is upregulated by exercise (14) and controls oxidative metabolism in both skeletal and cardiac muscle (15, 16), may be downstream of muscle IL-13–Stat3 signaling. RNA-seq data (validated by real-time PCR) demonstrated that exercise-induced muscle expression of *Esrra* and *Esrrg* was IL-13-dependent (Fig. 6C). Furthermore, adIL-13 increased *Esrra* and *Esrrg* in the quadriceps of *Stat3*$^{f/f}$ but not skm*Stat3*$^{-/-}$ mice (Fig. 6D). Putative Stat3-binding sites were identified ~2 kb upstream of the transcriptional initiation site for both *Esrra* and *Esrrg* genes (fig. S6H). The overexpression of *Stat3* in AD293 cells was sufficient to increase the 2-kb reporter activity of either *Esrra* or *Esrrg* in a dose-dependent manner (Fig. 6E and fig. S6I), but not the 1-kb promoter that lacked Stat3-binding sites. Mutation of the only Stat3-binding site in the *Esrrg* promoter abolished Stat3 regulation (Fig. 6E). To examine the regulation in a relevant cell type, *Stat3*$^{-/-}$ C2C12 myoblasts were generated through CRISPR/Cas9. rIL-13 increased luciferase activity of the 2-kb promoter in control but not *Stat3*$^{-/-}$ myoblasts (Fig. 6F and fig. S6J). The introduction of *Stat3* in *Stat3*$^{-/-}$ myoblasts increased basal promoter luciferase activities and restored the sensitivity to rIL-13 treatment. Thus, IL-13 appears to act as a regulator of the adaptive metabolic response of muscle to exercise training. This occurs, in part, through a coordinated transcriptional program mediated by Stat3 and Errα/Errγ.

Discussion

Metabolic conditioning of muscle to endurance exercise enhances fatty acid utilization and mitochondrial respiration, while reserving glycogen utilization, as a strategy to sustain energy supply for prolonged physical activity (17) (fig. S6K). This coordinated effort extends metabolic flexibility/efficiency, which contributes to the beneficial effects of exercise on health. In the current study, we demonstrate the interplay between immune and metabolic pathways through IL-13 signaling in the control of energy substrate utilization in endurance exercise. IL-13 acts directly on muscle cells to increase fatty acid oxidation and

mitochondrial ETC complex activity that is dependent on the downstream effector Stat3. Among the targets of the IL-13–Stat3 signaling are *Esrra* and *Esrrg*, two nuclear receptors also known to control fat catabolism and mitochondrial respiration in muscle (15, 18). A previous study examining Errα/Errγ cistromes in mitochondrial oxidative metabolism using ChIP-seq has predicted Stat3 binding sites co-localized with those occupied by Errs (19), implicating a feedforward mechanism for robust transcriptional outputs. Errα/Errγ are "orphan" nuclear receptors without well-defined endogenous ligands (20). How these receptors are activated remains unclear. Our results suggest that IL-13 may function as an upstream signal of the Stat3–Err transcriptional network.

Several lines of evidence indicate that IL-13 fits the criteria of a humoral factor mediating the metabolic benefits of exercise training. Endurance exercise increases circulating IL-13 levels in both women and men. rIL-13 treatment increases the uptake of glucose and fatty acid in myotubes. In mice, exercise-induced mitochondrial biogenesis and glucose homeostasis require IL-13 signaling. Furthermore, elevated IL-13 signaling in muscle drives exercise-like metabolic effects. IL-13 is not a classical myokine, since it is not produced by the muscle. One potential source of IL-13 is ILC2s. In concert, exercise leads to a higher percentage of ILC2 in the $CD45^+$ cell population in mouse muscle. Although IL-13-mediated Stat3 phosphorylation could be observed after a single exercise session, a significant increase in muscle IL-13 levels is achieved after training. This indicates that IL-13 signaling is induced immediately after exercise to modulate substrate utilization and stabilized by endurance training to mediate mitochondrial biogenesis.

Both ILC2 and IL-13 play important functions in the immune response to parasitic worms. Interestingly, prior infection with helminths in humans is associated with a higher VO_2 max (21), which is indicative of mitochondrial oxidative capacity and a predictor of running fitness. Thus, the coevolution of helminths and hosts may have resulted in increased metabolic efficiency in the latter, perhaps in response to the increased metabolic burden from parasite infection. Thus, IL-13 signaling may have evolved to regulate metabolic adaptation to energy stress during various states including parasitic infection, endurance exercise, and exposure to cold temperatures (22).

Methods summary

IL-13 levels were measured in plasma from sedentary and exercise-trained humans subjects and C57BL/6J mice. IL-13–producing ILC2s in mouse muscle after endurance training were identified by flow cytometry. *Il13*$^{-/-}$ mice in the C57BL/6J background were used to determine the role of IL-13 in muscle substrate utilization and mitochondrial respiration, running capacity and metabolic adaptation to endurance exercise. RNA-seq analyses were performed to identify IL-13-dependent, exercise-regulated metabolic programs in muscle. C2C12 myotubes were used for in vitro analysis of the effects of IL-13 signaling on energy metabolism and mitochondrial function. Skeletal muscle-specific *Il13ra1*$^{-/-}$ and *Stat3*$^{-/-}$ mice were generated to examine direct actions of IL-13 signaling in muscle. Intramuscular injection of adenoviral IL-13 was employed to increase IL-13 levels in skeletal muscle for gain-of-function studies.

Supplementary Material

Refer to Web version on PubMed Central for supplementary material.

Acknowledgments:

We thank Drs. G. Hotamisligil, R. V. Farese, and K. Inouye for help with treadmill/metabolic cage studies; Drs. A. J. Wagers, J. R. Mitchell, and X. Yang for critical comments; Drs. U. Unluturk and A. E. McQueen for technical assistance; and the IMB Genomics Core and IMB Bioinformatics Service Core at Academia Sinica (Taipei, Taiwan) for sequencing and RNA-seq data analysis.

Funding: This work was supported by grants from NIH (F31DK107256 to N.H.K.; F31GM117854 to R.K.A.; R01DK113791 and R21AI131659 to C.H.L) and American Heart Association (16GRNT31460005 to C.H.L.). Y.H.L. was supported by funds from Ministry of Science and Technology, Taiwan.

References:

1. United States. Department of Health and Human Services, 2008 physical activity guidelines for Americans : be active, healthy, and happy!, ODPHP publication (U.S. Dept. of Health and Human Services, Washington, DC, 2008), pp. ix, 61 p.
2. Goldstein MS, Humoral nature of the hypoglycemic factor of muscular work. Diabetes 10, 232–234 (1961). [PubMed: 13706674]
3. Pedersen BK, Febbraio MA, Muscles, exercise and obesity: skeletal muscle as a secretory organ. Nat Rev Endocrinol 8, 457–465 (2012). [PubMed: 22473333]
4. Di Gregorio GB, Hensley L, Lu T, Ranganathan G, Kern PA, Lipid and carbohydrate metabolism in mice with a targeted mutation in the IL-6 gene: absence of development of age-related obesity. Am J Physiol Endocrinol Metab 287, E182–187 (2004). [PubMed: 15191885]
5. O'Neill HM et al., IL-6 is not essential for exercise-induced increases in glucose uptake. J Appl Physiol (1985) 114, 1151–1157 (2013). [PubMed: 23449935]
6. Neill DR et al., Nuocytes represent a new innate effector leukocyte that mediates type-2 immunity. Nature 464, 1367–1370 (2010). [PubMed: 20200518]
7. Mahlakoiv T et al., Stromal cells maintain immune cell homeostasis in adipose tissue via production of interleukin-33. Sci Immunol 4, (2019).
8. Spallanzani RG et al., Distinct immunocyte-promoting and adipocyte-generating stromal components coordinate adipose tissue immune and metabolic tenors. Sci Immunol 4, (2019).
9. Kuswanto W et al., Poor Repair of Skeletal Muscle in Aging Mice Reflects a Defect in Local, Interleukin-33-Dependent Accumulation of Regulatory T Cells. Immunity 44, 355–367 (2016). [PubMed: 26872699]
10. Rana BMJ et al., A stromal cell niche sustains ILC2-mediated type-2 conditioning in adipose tissue. J Exp Med 216, 1999–2009 (2019). [PubMed: 31248899]
11. Egan B, Zierath JR, Exercise metabolism and the molecular regulation of skeletal muscle adaptation. Cell Metab 17, 162–184 (2013). [PubMed: 23395166]
12. Orchansky PL, Kwan R, Lee F, Schrader JW, Characterization of the cytoplasmic domain of interleukin-13 receptor-alpha. J Biol Chem 274, 20818–20825 (1999). [PubMed: 10409622]
13. Stanya KJ et al., Direct control of hepatic glucose production by interleukin-13 in mice. J Clin Invest 123, 261–271 (2013). [PubMed: 23257358]
14. Rangwala SM et al., Estrogen-related receptor gamma is a key regulator of muscle mitochondrial activity and oxidative capacity. J Biol Chem 285, 22619–22629 (2010). [PubMed: 20418374]
15. Huss JM, Torra IP, Staels B, Giguere V, Kelly DP, Estrogen-related receptor alpha directs peroxisome proliferator-activated receptor alpha signaling in the transcriptional control of energy metabolism in cardiac and skeletal muscle. Mol Cell Biol 24, 9079–9091 (2004). [PubMed: 15456881]

16. Wang T et al., Estrogen-related receptor alpha (ERRalpha) and ERRgamma are essential coordinators of cardiac metabolism and function. Mol Cell Biol 35, 1281–1298 (2015). [PubMed: 25624346]
17. Overmyer KA et al., Maximal oxidative capacity during exercise is associated with skeletal muscle fuel selection and dynamic changes in mitochondrial protein acetylation. Cell Metab 21, 468–478 (2015). [PubMed: 25738461]
18. Narkar VA et al., Exercise and PGC-1alpha-independent synchronization of type I muscle metabolism and vasculature by ERRgamma. Cell Metab 13, 283–293 (2011). [PubMed: 21356518]
19. Dufour CR et al., Genome-wide orchestration of cardiac functions by the orphan nuclear receptors ERRalpha and gamma. Cell Metab 5, 345–356 (2007). [PubMed: 17488637]
20. Audet-Walsh E, Giguere V, The multiple universes of estrogen-related receptor alpha and gamma in metabolic control and related diseases. Acta Pharmacol Sin 36, 51–61 (2015). [PubMed: 25500872]
21. Pisor AC, Gurven M, Blackwell AD, Kaplan H, Yetish G, Patterns of senescence in human cardiovascular fitness: VO2 max in subsistence and industrialized populations. Am J Hum Biol 25, 756–769 (2013). [PubMed: 24022886]
22. Lee MW et al., Activated type 2 innate lymphoid cells regulate beige fat biogenesis. Cell 160, 74–87 (2015). [PubMed: 25543153]
23. Takeda K et al., Stat3 activation is responsible for IL-6-dependent T cell proliferation through preventing apoptosis: generation and characterization of T cell-specific Stat3-deficient mice. J Immunol 161, 4652–4660 (1998). [PubMed: 9794394]
24. Fontaine DA, Davis DB, Attention to Background Strain Is Essential for Metabolic Research: C57BL/6 and the International Knockout Mouse Consortium. Diabetes 65, 25–33 (2016). [PubMed: 26696638]
25. Stevenson JL et al., Echinacea-Based Dietary Supplement Does Not Increase Maximal Aerobic Capacity in Endurance-Trained Men and Women. J Diet Suppl 13, 324–338 (2016). [PubMed: 26317662]
26. Kim JH et al., Temporal Changes in Cardiovascular Remodeling Associated with Football Participation. Med Sci Sports Exerc 50, 1892–1898 (2018). [PubMed: 29634639]
27. Shalem O et al., Genome-scale CRISPR-Cas9 knockout screening in human cells. Science 343, 84–87 (2014). [PubMed: 24336571]
28. Sanjana NE, Shalem O, Zhang F, Improved vectors and genome-wide libraries for CRISPR screening. Nat Methods 11, 783–784 (2014). [PubMed: 25075903]
29. Narkar VA et al., AMPK and PPARdelta agonists are exercise mimetics. Cell 134, 405–415 (2008). [PubMed: 18674809]
30. Bonetto A, Andersson DC, Waning DL, Assessment of muscle mass and strength in mice. Bonekey Rep 4, 732 (2015). [PubMed: 26331011]
31. Gruntman AM et al., Gene transfer in skeletal and cardiac muscle using recombinant adeno-associated virus. Curr Protoc Microbiol Chapter 14, Unit 14D 13 (2013).
32. Boutagy NE et al., Isolation of Mitochondria from Minimal Quantities of Mouse Skeletal Muscle for High Throughput Microplate Respiratory Measurements. J Vis Exp, (2015).
33. Jacobi D et al., Hepatic Bmal1 Regulates Rhythmic Mitochondrial Dynamics and Promotes Metabolic Fitness. Cell Metab 22, 709–720 (2015). [PubMed: 26365180]

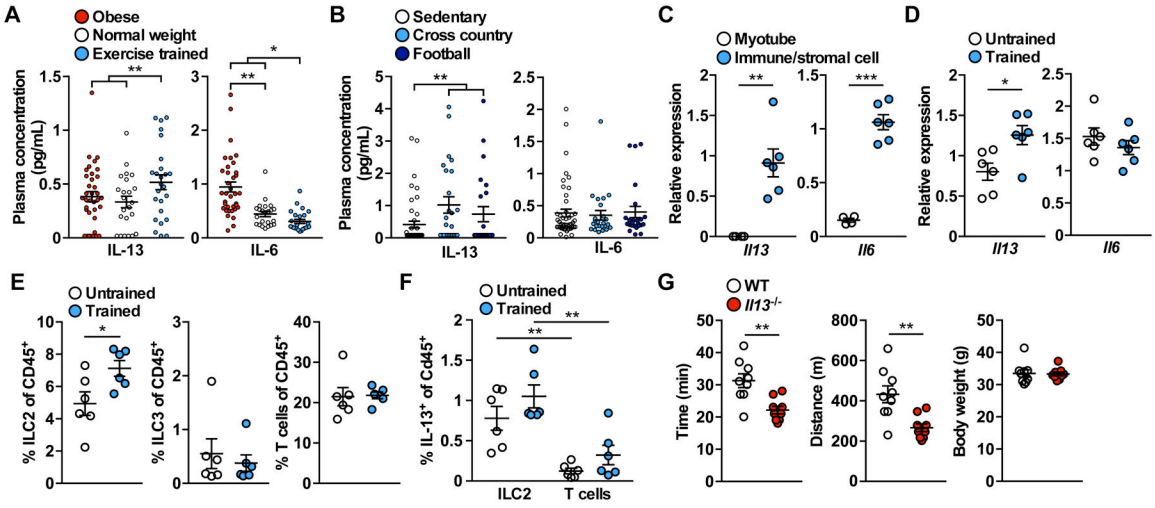

Fig. 1. IL-13 is an exercise-inducible factor regulating endurance capacity

(A) Resting plasma concentrations of IL-13 and IL-6 in sedentary (n=36 obese; n=23 normal weight) and exercise-trained (n=25) women. Linear regressions were used to examine associations adjusting for age and obesity status. Detailed data are in table S1. (B) Resting plasma concentrations of IL-13 and IL-6 in normal-weight sedentary controls (n=48) and exercise-trained men (n=25 cross-country; n=24 football). Linear regressions were used to examine associations adjusting for age and training type. Detailed data are in table S2. (C) mRNA expression of *Il13* and *Il6* in primary myotubes (differentiated from primary myoblasts or satellite cells) or muscle immune/stromal cells (Percoll gradient-isolated) measured by qPCR. n=4–6/group, experiment performed twice, statistical analysis performed using unpaired Student's *t*-test. (D) mRNA expression of *Il13* and *Il6* in muscle immune/stromal cells from untrained or 4-week endurance–trained mice measured by qPCR. n=6/group, experiment performed twice, statistical analysis performed using unpaired Student's *t*-test. (E) Quantification of % ILC2 (Gata3$^+$), ILC3 (Rorγt$^+$), and T cells (CD3$^+$) among CD45$^+$ cells in skeletal muscle of untrained or 4-week endurance–trained mice. n=6/group, 10-week-old male mice, experiment performed twice, statistical analysis performed using unpaired Student's *t*-test. (F) Quantification of % IL-13$^+$ ILC2 (Gata3$^+$) and T cells (CD3$^+$) among CD45$^+$ cells in skeletal muscle of untrained or 4-week endurance–trained mice. n=6/group, 10-week old male mice, experiment performed twice, statistical analysis performed using unpaired Student's *t*-test. (G) Endurance capacity test performed by treadmill running in WT and *Il13*$^{-/-}$ mice. n=9/group, 16-week-old male mice, experiment performed four times, statistical analysis performed using unpaired Student's *t*-test. Additional mouse cohort data included in table S3. Error bars indicate SEM. *p<0.05, **p<0.01, ***p<0.001.

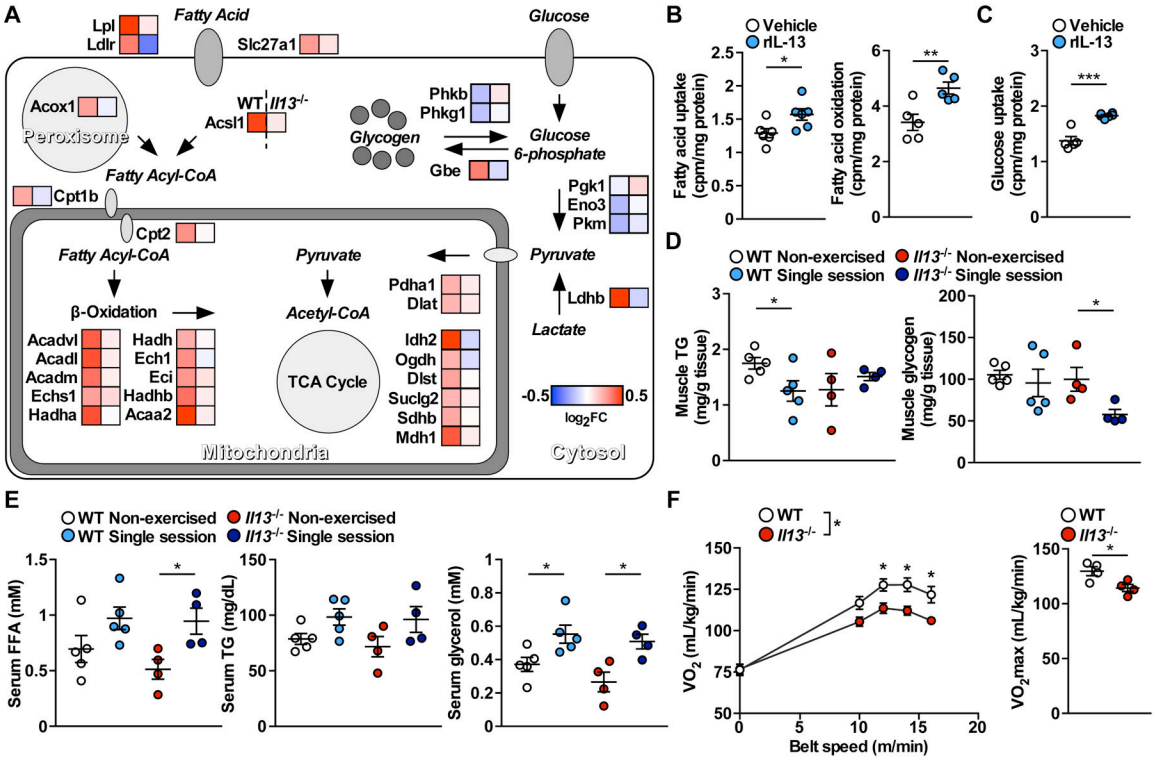

Fig. 2. IL-13 regulates metabolic substrate utilization in exercising muscle.

(A) Illustration of key metabolic genes in muscle metabolism regulated by endurance training in gastrocnemius of WT and *Il13*$^{-/-}$ mice identified by RNA-seq. Data presented as heatmap (log_2-fold change, trained versus untrained of the same genotype) with WT animals on the left and *Il13*$^{-/-}$ on the right. Red indicates higher expression in exercised muscle, whereas blue indicates lower expression. n=4/group, 20-week-old male mice. (B) Fatty acid uptake and oxidation and (C) glucose uptake in C2C12 myotubes treated with rIL-13 (10 ng/mL) overnight. n=5–6 biological replicates/group/experiment, experiment performed four times, statistical analysis performed using unpaired Student's *t*-test. (D) Triglyceride (TG) and glycogen levels in the quadriceps of non-exercised (control) and single-session exercised, WT and *Il13*$^{-/-}$ mice. n=4–5/group, 24-week-old male mice, experiment performed twice, statistical analysis (non-exercise vs single-session of the same genotype) performed using unpaired Student's *t*-test. (E) Serum concentrations of free fatty acids (FFA), triglyceride (TG) and glycerol in control and single-session exercised, WT and *Il13*$^{-/-}$ mice. n=4–5/group, 24-week-old male mice, experiment performed twice, statistical analysis (non-exercise vs single-session of the same genotype) performed using unpaired Student's *t*-test. (F) Respiration of exercising WT and *Il13*$^{-/-}$ mice at increasing running speeds. Maximum oxygen uptake (VO_2 max) under the experimental setting was assessed and shown in the right panel. n=4/group, 24-week-old female mice, experiment performed twice, statistical analysis performed using two-way ANOVA with Bonferroni post-hoc test with animal group and time points modeled as variables (respiration) and unpaired Student's *t*-test (VO_2 max). Error bars indicate SEM. *p<0.05, **p<0.01, ***p<0.001.

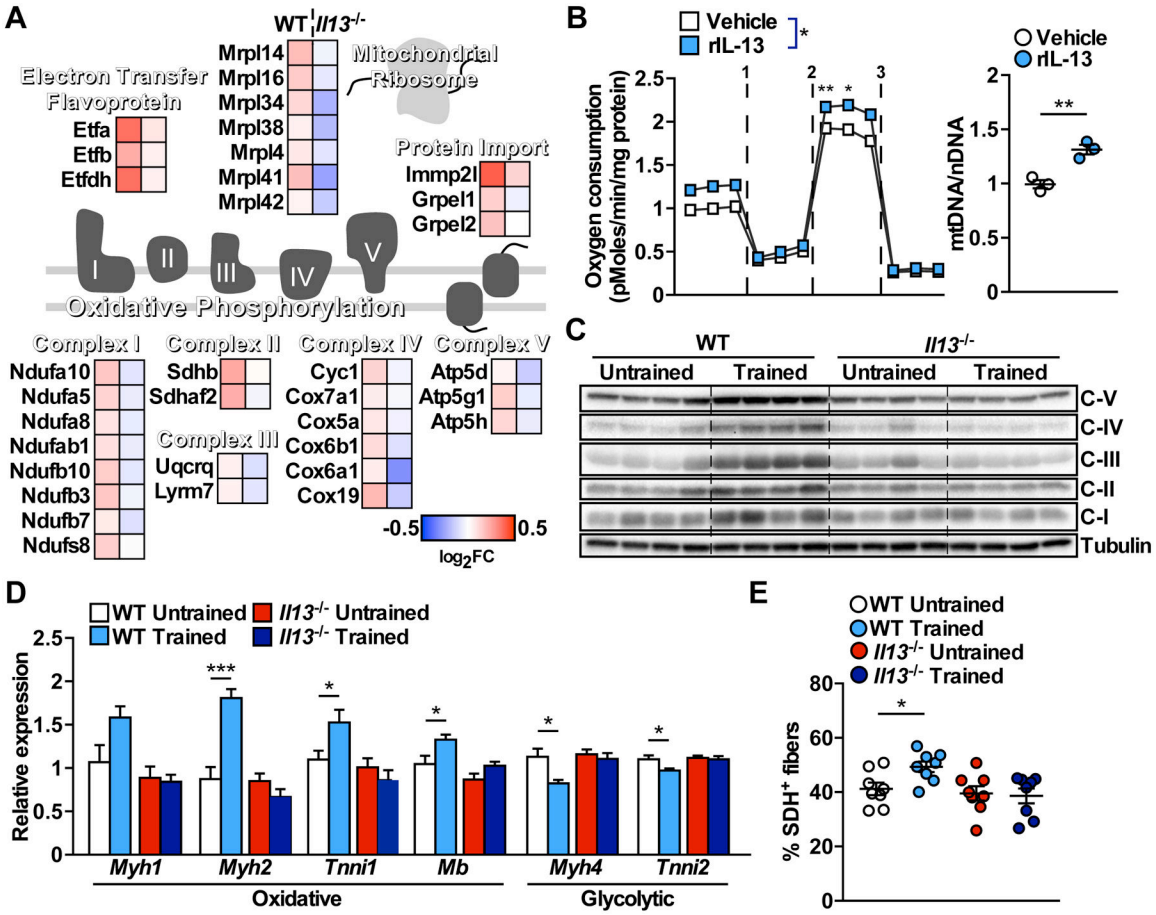

Fig. 3. Mitochondrial biogenesis in endurance-trained muscle requires IL-13 signaling.

(A) Representative mitochondrial genes differentially regulated in the gastrocnemius of endurance-trained WT and *Il13*$^{-/-}$ mice identified by RNA-seq. Data presented as a heatmap ($\log_2$-fold change, trained versus untrained of the same genotype) with WT animals on the left and *Il13*$^{-/-}$ on the right. Red indicates higher expression in exercised muscle, whereas blue indicates lower expression. n=4/group, 20-week-old male mice. (B) Left panel: mitochondrial respiration of C2C12 myotubes treated with rIL-13 (10 ng/mL) overnight. Oligomycin (1) was added to block ATP-coupled respiration, FCCP (2) to induce maximal respiration, and antimycin A/rotenone (3) to block mitochondrial electron transport. n=5 biological replicates/group/experiment, experiments performed six times, statistical analysis performed using two-way ANOVA with Bonferroni post-hoc test with treatment and time points modeled as variables. Right panel: mtDNA content of C2C12 myotubes treated with rIL-13 (10 ng/mL) overnight. Relative mitochondrial DNA (mtDNA) content was measured by qPCR normalized to nuclear DNA (nDNA). n=3 biological replicates/group/experiment, experiments performed six times, statistical analysis performed using unpaired Student's *t*-test. (C) Immunoblot analyses of gastrocnemius mitochondrial protein content from untrained and endurance-trained WT and *Il13*$^{-/-}$ mice. n=4/group, experiment performed twice, 20-week-old male mice. (D) mRNA expression of oxidative and glycolytic muscle fiber type markers measured by qPCR in gastrocnemius muscle from untrained and endurance-trained WT and *Il13*$^{-/-}$ mice. n=6–7/group, 20-week-old male mice, experiment

performed three times, statistical analysis (untrained vs trained of the same genotype) performed using unpaired Students *t*-test. (E) Quantification of succinate dehydrogenase positive (SDH^+) muscle fibers in cross-sections of gastrocnemius from untrained and endurance-trained WT and *Il13*$^{-/-}$ mice. n=8/group, 20-week-old male mice, experiment performed twice, statistical analysis (untrained vs trained of the same genotype) performed using unpaired Student's *t*-test. Error bars indicate SEM. *p<0.05, **p<0.01, ***p<0.001.

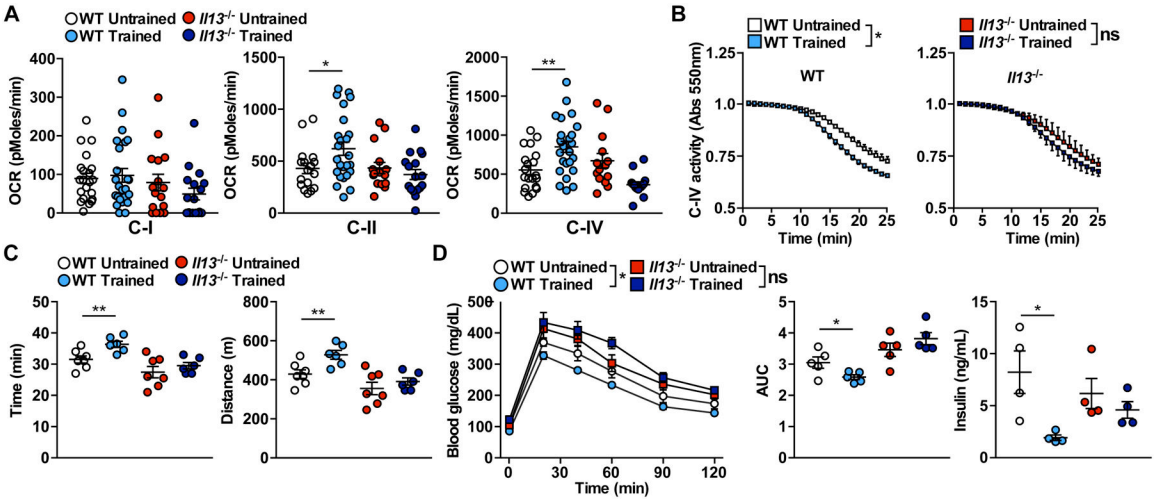

Figure 4. Endurance training increases running capacity and glucose tolerance via IL-13 signaling.

(A) Electron flow assay using Seahorse bioanalyzer with mitochondria isolated from gastrocnemius of untrained and endurance-trained WT and *Il13*$^{-/-}$ mice. Complex I (C-I) respiration was measured using pyruvate and malate as substrates and blocked with rotenone. Complex II (C-II) was measured using succinate as substrate and blocked with antimycin A. Complex IV (C-IV) respiration was measured by injecting tetramethyl-*p*-phenylenediamine/ascorbate. n=15–25 replicates/group, data combined from three experiments, statistical analysis (untrained vs trained of the same genotype) performed using unpaired Student's *t*-test. (B) Complex IV activity assay performed with gastrocnemius mitochondria from untrained and endurance-trained WT and *Il13*$^{-/-}$ mice. The activity was assessed by the rate of cytochrome c oxidation measured by the decline in reduced cytochrome c (absorbance at 550 nm). n=3–5/group, 20-week-old female mice, experiment performed twice, statistical analysis performed using two-way ANOVA with Bonferroni post-hoc test with animal group and time points modeled as variables. (C) Endurance capacity test performed by treadmill running in untrained and endurance-trained WT and *Il13*$^{-/-}$ mice. n=6–7/group, 16-week-old male mice, experiment performed twice, statistical analysis (untrained vs trained of the same genotype) performed using unpaired Student's *t*-test. (D) Left panel: glucose tolerance test (GTT) of untrained and endurance-trained WT and *Il13*$^{-/-}$ mice. Middle panel: area under the curve (AUC) of the GTT. Right panel: fasting serum insulin levels of untrained and endurance-trained WT and *Il13*$^{-/-}$ mice. n=5/group for GTT/AUC and n=4/group for serum insulin, 20-week-old male mice, experiment performed three times, statistical analysis (untrained vs trained of the same genotype) performed using two-way ANOVA with Bonferroni post-hoc test with animal group and time points modeled as variables (GTT) and unpaired Student's *t*-test (AUC and serum insulin). Error bars indicate SEM. *p<0.05, **p<0.01, ***p<0.001.

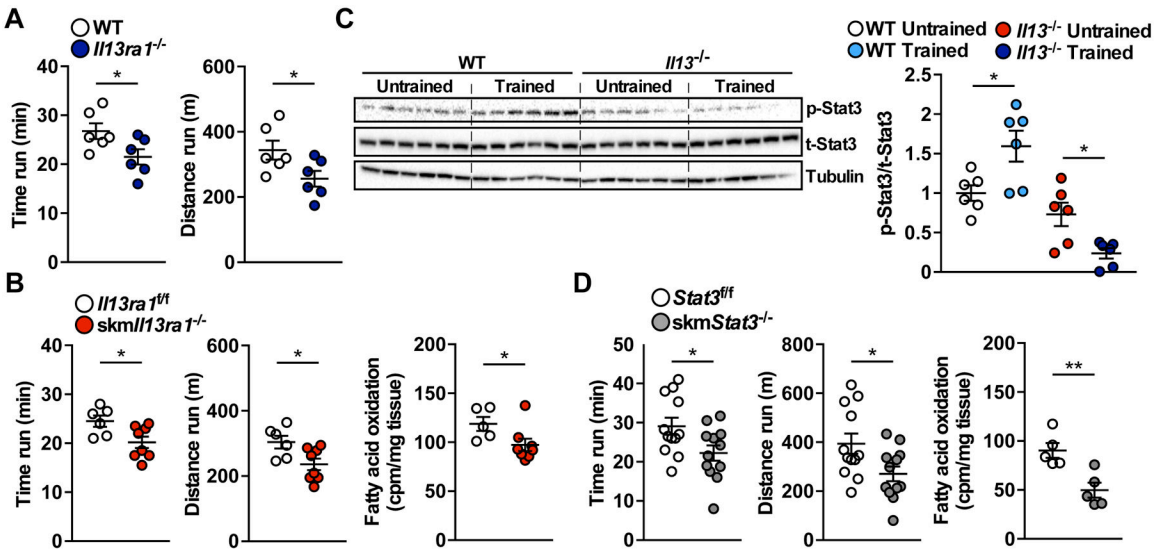

Fig. 5. IL-13Rα1 and Stat3 are downstream effectors of IL-13 in muscle.

(A) Endurance capacity test of WT and *Il13ra1*$^{-/-}$ mice performed by treadmill running. n=6/group, 20-week-old male mice, experiment performed twice, statistical analysis performed using unpaired Student's *t*-test. (B) Endurance capacity test performed by treadmill running and ex vivo fatty acid oxidation of isolated soleus muscle from *Il13ra1*$^{f/f}$ (control) and skm*Il13ra1*$^{-/-}$ mice. n=6–8/group (endurance capacity) and n=5–8/group (fatty acid oxidation), 24-week-old male mice, experiment performed twice, statistical analysis performed using unpaired Student's *t*-test. (C) Immunoblot analyses and quantification of Stat3 phosphorylation (Y705) in quadriceps muscle of untrained and endurance-trained WT and *Il13*$^{-/-}$ mice. n=6/group, 16-week-old female mice, experiment performed three times, statistical analysis (untrained vs trained of the same genotype) performed using unpaired Student's *t*-test. p-Stat3: phospho-Stat3; t-Stat3: total-Stat3. (D) Endurance capacity test performed by treadmill running and ex vivo fatty acid oxidation of isolated soleus muscle from *Stat3*$^{f/f}$ (control) and skm*Stat3*$^{-/-}$ mice. n=12/group for endurance capacity and n=5/group for fatty acid oxidation, 24-week-old male mice, experiment performed twice, statistical analysis performed using unpaired Student's *t*-test. Error bars indicate SEM. *p<0.05, **p<0.01.

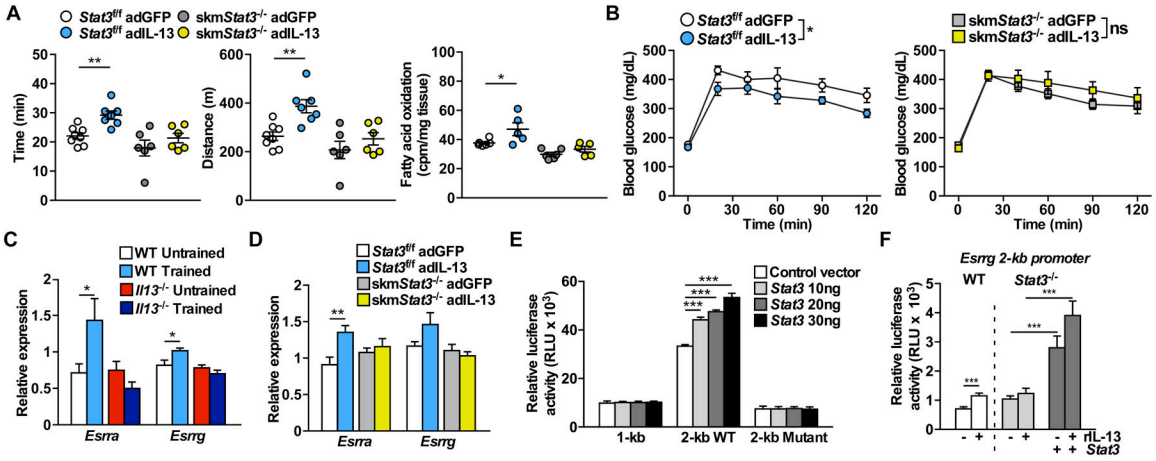

Figure 6. Increased IL-13 signaling in muscle drives a Stat3-dependent, exercise-like effect.

(A) Endurance capacity test performed by treadmill running of *Stat3*$^{f/f}$ and skm*Stat3*$^{-/-}$ mice injected with adGFP or adIL-13 into gastrocnemius muscle. n=6–8/group, 24-week-old male mice, experiment performed twice, statistical analysis (adGFP vs adIL-13 of the same genotype) performed using unpaired Student's *t*-test. Right panel: Ex vivo fatty acid oxidation of isolated soleus muscle from *Stat3*$^{f/f}$ and skm*Stat3*$^{-/-}$ mice injected with adGFP or adIL-13 into gastrocnemius muscle. n=5–6/group, 24-week-old male mice, experiment performed once, statistical analysis (adGFP vs adIL-13 of the same genotype) performed using unpaired Student's *t*-test. (B) Glucose tolerance test (GTT) of mice injected with adGFP or adIL-13 into gastrocnemius muscle. n=6–8/group, 24-week-old male mice, experiment performed twice, statistical analysis performed using two-way ANOVA with Bonferroni post-hoc test with animal group and time points modeled as variables. (C) mRNA expression of *Esrra* and *Esrrg* in gastrocnemius muscle of untrained and endurance-trained WT and *Il13*$^{-/-}$ mice measured by qPCR. n=6–7/group, 20-week-old male mice, experiment performed twice, statistical analysis (untrained vs trained of the same genotype) performed using unpaired Student's *t*-test. (D) mRNA expression of *Esrra* and *Esrrg* in quadriceps muscle of *Stat3*$^{f/f}$ and skm*Stat3*$^{-/-}$ mice after gastrocnemius injection of adGFP or adIL-13 measured by qPCR. n=6–8/group, 24-week-old males, experiment performed once, statistical analysis (adGFP vs adIL-13 of the same genotype) performed using unpaired Student's *t*-test. (E) Stat3 regulation of *Esrrg* gene promoter in reporter transient transfection assays. Relative luciferase activity of reporters driven by *Esrrg* promoters in AD293 cells co-transfected with increasing amounts of *Stat3* expression vector. "1-kb", "2-kb WT", and "2-kb mutant" refer to reporter constructs containing 1-kb, 2-kb, and 2-kb with the mutated Stat3 binding site of *Esrrg* promoter, respectively. n=6 biological replicates/group/experiment, experiment performed four times, statistical analysis performed using unpaired Student's *t*-test. (F) Relative luciferase activity of 2-kb *Esrrg* promoter in WT and *Stat3*$^{-/-}$ C2C12 myoblasts. *Stat3*$^{-/-}$ cells were co-transfected with a control or *Stat3* expression vector ± rIL-13 overnight. n=12 biological replicates/group/experiment, experiment performed three times, statistical analysis performed using unpaired Student's *t*-test. Error bars indicate SEM. *p<0.05, **p<0.01, ***p<0.001.